Energy barrier of magnetization reversal in a magnetic wire with defects

Yuejin Zhu,[1] Xian Yu,[1] and Shufeng Zhang[1,2]

[1]*Department of Physics, Ningbo University, Ningbo 315211, People's Republic of China*
[2]*Department of Physics, University of Arizona, Tucson, Arizona 85721, USA*

We consider the energy barrier to magnetization reversal in a one-dimensional (1D) magnetic wire with defects. By solving the variable coefficient double Sine-Gordon equation, we obtain the dependence of the energy barrier on the strength and the range of a defect potential. We find that there is a minimum-energy barrier for two defects placed at an optimal distance which is correlated with the width of a 360° untwisted domain wall. The possible experimental realization of our results is discussed.

I. INTRODUCTION

Thermal stability of a magnetic bit, which is determined by the ratio of the energy barrier E_b to the thermal fluctuation $k_B T$,[1] is an important issue in magnetic storage devices. Due to complexity of the magnetization reversal process, there are very few examples where the energy barrier can be analytically derived. For a single-domain particle, the calculation of the energy barrier is trivial because the magnetic energy only depends on the orientation of the magnetization vector and all equilibrium states can be readily obtained.[2] For nonsingle domain magnetic reversal, the task of finding the energy barrier is much more challenging since there are infinite numbers of reversal configurations.

The simplest example for the nonsingle domain energy barrier is a long magnetic wire where the direction of the magnetization depends only on one spatial coordination x, i.e., $\mathbf{M}(x)$. The thermal stability of a magnetic bit based on the magnetic wire has been considered robust due to the shape anisotropy in addition to the crystalline anisotropy.[3] For an ideal wire, the energy barrier would be proportional to $K_e V$ for a uniform coherent rotation, where K_e are the anisotropies and V is the volume of the entire wire. Braun[4,5] showed that the energy barrier through the nucleation of an untwist 360° domain wall, which can be mathematically described by the solitons of the double Sine-Gordon model, could be much lower because the energy barrier is now proportional to the size of the wall instead of the total volume of the wire. Another similar example is the ideal ring-shaped magnet where the magnetization reversal and the energy barrier in the presence of the circular magnetic field were investigated.[6] For these ideal wires or rings, due to translational or rotational invariance of the structure, the double solitons (360° domain walls) can be located at any point. In experimental wires, however, the presence of wire/ring roughness and defects breaks the symmetry. Recently, Loxley[7] considered the effect of a localized defect in an otherwise ideal wire and found that the nucleation can take several different modes depending on the strength of the defect. In general, defects reduce the energy needed for the nucleation of the domain wall and thus suppressing the thermal stability.

Recent experimental advances[8–13] in fabrication and characterization of engineered magnetic wires with controlled defects make it possible to quantitatively compare experimental results with theoretical calculations. Since there are always defects for experimental wires, we will investigate the dependence of the energy barrier on the strength and the range of defect potentials. For a given defect potential, we solve the generalized Sine-Gordon equation by a finite-difference method based on the trial function established by Braun.[4,5] This paper is organized as follows. In Sec. II, we briefly outline our model and discuss the results for the ideal wire. Then we present the dependence of the energy barrier on the strength and the range of the defect potential by numerically solving the model equation. In Sec. IV, we consider the effect of two defects. We show that there is an energy barrier minimum when two defects are placed at an optimal distance. We summarize and conclude our paper in Sec. V.

II. MODEL

We consider an infinitely long one-dimensional (1D) wire with the following total magnetic energy:

$$\epsilon = \int_{-\infty}^{\infty} dx \left\{ \frac{A}{M_s^2} [(\partial_x M_x)^2 + (\partial_x M_y)^2 + (\partial_x M_z)^2] \right.$$
$$\left. + \frac{K_h}{M_s^2} M_z^2 - \frac{K_e}{M_s^2} M_x^2 - \frac{K_d}{M_s^2} M_y^2 - H_{\text{ext}} M_x \right\}, \quad (1)$$

where A is the exchange stiffness, M_s is the saturation magnetization, K_h is the in-plane anisotropy constant, K_e is the easy-axis uniaxial anisotropy, $K_d = K_d(x)$ is a defect potential which reduces easy-axis anisotropy but enhances the easy-plane anisotropy, and H_{ext} is the external field. If we use the spherical coordination for the magnetization vector $\mathbf{M} = M_s(\sin\theta\cos\phi, \sin\theta\sin\phi, \cos\theta)$ and define the reduced units for the length $[x] = \sqrt{A/K_e}$, the energy $[\epsilon] = 2\sqrt{AK_e}$, the defect potential $a_d = K_d/K_e$, the in-plane anisotropy ratio $Q = K_e/K_h$, and the applied field $h = H_{\text{ext}} M_s/(2K_e)$, Eq. (1) can be written in the unitless form

$$\epsilon = \int_{-\infty}^{\infty} dx \left\{ \frac{1}{2} [(\partial_x \theta)^2 + \sin^2\theta(\partial_x \phi)^2] - \frac{1-a_d}{2} [\sin^2\theta\cos^2\phi - 1] \right.$$
$$\left. + \frac{Q^{-1} + a_d}{2} \cos^2\theta - h\sin\theta\cos\phi \right\}. \quad (2)$$

The most interesting case is the large in-plane anisotropy

144411-1

limit, i.e., $Q^{-1} \to \infty$, so that we can immediately place the magnetization in the plane $\theta = \pi/2$. We shall only discuss this limit case throughout the paper; the finite Q^{-1} would considerably increase the complexity of the calculation which will be the subject for later study.

The equilibrium states can be found by $\delta\epsilon/\delta\phi = 0$. From Eq. (2), we have

$$-\frac{d^2\phi}{dx^2} + [1 - a_d]\sin\phi\cos\phi + h\sin\phi = 0. \qquad (3)$$

The above equation determines all equilibrium states including the ground state, metastable states, as well as the saddle points for the magnetization reversal. Once we determine the saddle-point solution $\phi = \phi_s(x)$ from the above equation, we can evaluate the energy barrier for $h > 0$,

$$\begin{aligned} E_b &= \epsilon(\phi_s) - \epsilon(\phi = \pi) \\ &= \int_{-\infty}^{\infty} dx \left[\frac{1}{2}\left(\frac{d\phi_s}{dx}\right)^2 + \frac{(1-a_d)}{2}\sin^2\phi_s - h(1 + \cos\phi_s) \right], \end{aligned}$$
$$(4)$$

where we assume that the magnetization vector is initially at $\phi = \pi$ metastable state. In the absence of the defect, $a_d = 0$, Braun[4] found two nonuniform solutions. One solution is

$$\phi_s^t(x) = 2\tan^{-1}\left[\frac{\cosh R_b}{\sinh(x/\delta_b)}\right], \qquad (5)$$

where R_b and δ_b are determined by the magnetic field $h = \text{csch}^2 R_b$ and $\delta_b = \tanh R_b$ and describe two twisted π walls separated by $\delta_b R_b$; this solution is stable against small perturbations and thus it is not a saddle point. The other solution is

$$\phi_s^u(x) = 2\tan^{-1}\left[\frac{\cosh(x/\delta_s)}{\sinh R_s}\right], \qquad (6)$$

where R_s and δ_s are similarly determined by the magnetic field $h = \text{sech}^2 R_s$ and $\delta_s = \coth R_s$ and describe two untwisted π walls also separated by $\delta_s R_s$; this is a saddle point whose energy barrier relative to the metastable state ($\phi_s = \pi$) is

$$E_b = 4\tanh R_s - 4R_s \, \text{sech}^2 R_s. \qquad (7)$$

In the presence of a highly localized state at $x = 0$, $a_d = B\delta(x)$, Loxley[7] extended Braun's solution by constructing a superposition of Braun's functions [Eq. (6)] for $x > 0$ and $x < 0$ and by using the boundary condition at $x = 0$ to determine the coefficients. We will first consider below one defect with a finite range L and strength V_0 such that

$$a_d(x) = V_0 \exp(-x^2/L^2). \qquad (8)$$

While the above defect potential is introduced rather arbitrarily, it should roughly model an experimental case where one makes a notch at the edge of an ideal wire.[14] Due to strong magnetostatic interaction, the notch generates a pinning potential. One may approximately correlate the size and the strength of the pinning potential by the width (parallel to the wire) and the depth (perpendicular to the wire) of the notch.
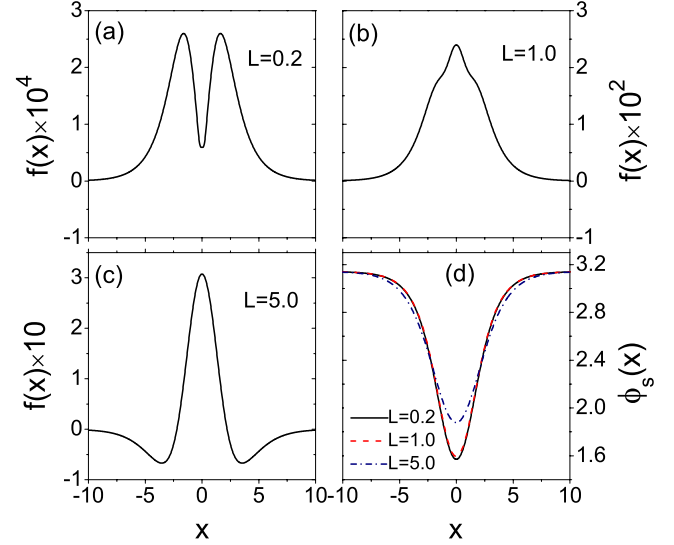

FIG. 1. (Color online) The solution of $f(x)$ for three different defect sizes (a) $L = 0.2$, (b) 1, and (c) 5, where the field $h = 0.5$ and the defect potential $V_0 = 0.3$ are fixed. (d) The magnetization direction $\phi_s(x) = \phi_s^u(x) + f(x)$ for the above three cases.

Since the double Sine-Gordon model [Eq. (3)] has many solutions in general, a direct numerical integration of Eq. (3) is usually unable to find our interested saddle-point solution. Instead, we should first choose a trial function which is near the vicinity of the saddle point. Since the saddle point of the ideal wire is already known [Eq. (6)], we conveniently consider the solution in the form

$$\phi_s(x) = \phi_s^u(x) + f(x), \qquad (9)$$

where $\phi_s^u(x)$ is given by Eq. (6). By placing Eq. (9) into Eq. (3), we obtain the second-order nonlinear differential equation for the function $f(x)$. By using nonlinear finite-difference method[15] for solving differential equations, we find that the function $f(x)$ behaves normally and the deviation of $\phi_s(x)$ from $\phi_s^u(x)$ is always small for all the defect potentials we are interested in. Similar to the argument of $\phi_s^u(x)$ being the saddle point for the ideal wire, our solution $\phi_s(x)$ described below is also a saddle point for the magnetic wire with defects.

III. ENERGY BARRIERS

When the defect potential or the applied magnetic field is large ($V_0 \gg 1$ or $h > 1$), the initial metastable state $\phi = \pi$ becomes unstable. In this case, the magnetization either spontaneously forms domain structures to minimize the energy or completely reverses its direction to $\phi = 0$. Since we are only interested in the energy between the saddle point and the metastable state of $\phi = \pi$, we should limit the magnetic field to $0 < h < 1$ and the defect potential to $V_0 < 1$. In Fig. 1, we show the solution of the magnetization for three different values of the defect potential size L for a fixed field $h = 0.5$ and the potential strength $V_0 = 0.3$. We have seen that the correction $f(x)$ to the defect-free domain wall $\phi_s^u(x)$ is small in all cases. $f(x)$ becomes sizable for the large-size defect
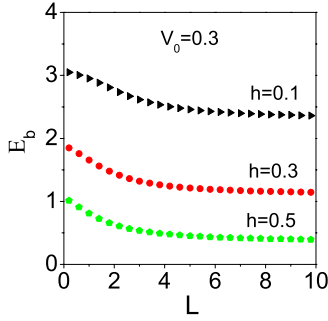
FIG. 2. (Color online) The energy barrier as a function of defect size for a fixed defect potential $V_0=0.3$ for three different magnetic fields.

$L=5$. The energy barrier decreases as the defect size increases; this is largely expected. As shown in Fig. 2, the energy barrier decreases when the defect size continuously increases to the several times of the domain-wall width. Further increase in the size of the defect does not change the energy barrier anymore. This is consistent with Fig. 1 illustrating that the function $\phi_s(x)$ is a localized function whose range is a few times of the domain-wall width; thus, the defect potential outside this range does not affect the energy barrier.

Figure 3 shows the variation in the energy barrier with respect to the strength of the defect potential. When the defect size is small, the energy barrier is nearly independent of the potential strength up to $V_0=1$. When the defect size is comparable to the domain-wall width $L=1$, the energy barrier remains unaffected for a small field but decreases considerably at the large field; this could be understood in terms of the field dependence of the domain-wall width: the larger the field is, the narrower the wall is. Thus, the large field makes the defect size larger than the domain-wall width and produces a stronger effect on the energy barrier. In the case of a large defect size, $L=5$, the energy barrier depends on the strength of the defects for all applied fields. Interestingly,
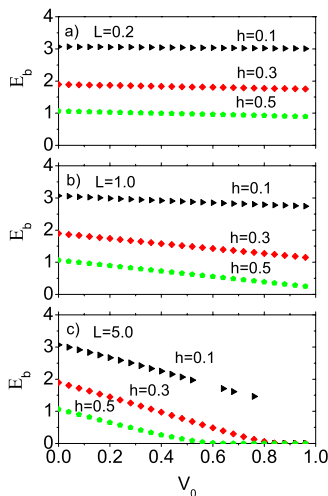

FIG. 3. (Color online) The energy barrier as a function of the defect potential strength for various magnetic fields and the defect sizes of (a) $L=0.2$, (b) 1, and (c) 5.
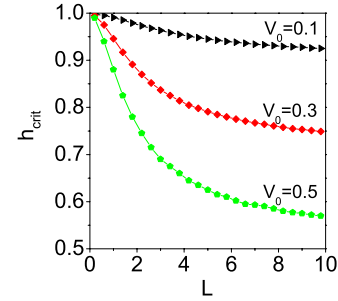
when the defect strength or the magnetic field is large enough, the energy barrier is reduced to zero; i.e., magnetization reversal occurs.

To quantitatively address the disappearance of the energy barrier, we show in Fig. 4 the critical magnetic field h_{crit} where the energy barrier reaches zero. The critical field h_{crit} decreases exponentially as one increases the strength and the size of the defect potential, and it reaches a saturation for large L.

FIG. 4. (Color online) The critical magnetic field h_{crit} as a function of the defect potential size for various defect potential strengths.

IV. ENERGY BARRIERS WITH TWO DEFECTS

Having quantitatively calculated the dependence of the energy barrier on the defect potential, the size, and the applied magnetic field for a single defect, we consider the effect of two defects. The multiple defects either exist naturally in a realistic film or can be grown purposely by making geometric notches at the edges of the film.[14] If we continue to assume the defect potential in the form of Eq. (8), we can write the total potential of the two defects as

$$a_d(x) = V_0\left[\exp\left(-\frac{(x-x_0)^2}{L^2}\right) + \exp\left(-\frac{(x+x_0)^2}{L^2}\right)\right],$$

(10)

where $2x_0$ is the separation of the centers of the two defect potentials. We have used the same numerical method[15] to solve Eq. (3) by using the above defect potential.

In Fig. 5, we show the dependence of the energy barrier on the separation of the two defects for a fixed magnetic field $h=0.1$ but different defect sizes and potentials. The energy barrier shows a minimum value, indicating the existence of an optimal distance between two defects to achieve minimum-energy barrier. Surprisingly, the optimal distance is almost independent of the defect potential size and strength. To explain this result, we draw the magnetization vector of the saddle-point untwisted wall in the absence of the defects [Fig. 6(a)]. Clearly, the untwisted wall has two locations where the magnetization vectors are perpendicular to the easy axis. If we place the two defects at these two locations, the energy reduction would be maximum; i.e., the energy barrier would be minimum if the separation of the defects matches Δ that is labeled in Fig. 6(a). Since Δ is very weakly dependent on the defect potential strength and size,
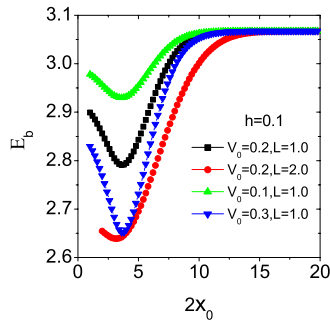
FIG. 5. (Color online) The energy barrier as a function of the separation of two defects for different defect size and potential strength. The magnetic field is fixed at $h=0.1$. Note that the minimum-energy barrier occurs at approximately the same $x_0=1.8$ for these curves.

FIG. 6. (Color online) (a) The magnetization vector of the saddle-point untwisted wall at h_{crit} in the absence of defects. The two locations with the magnetization vector perpendicular to the easy axis are labeled; their separation is Δ. (b) The optimal separation of the defects, and Δ as a function of the applied magnetic field.

this picture explains why the optimal separations are approximately the same.

To confirm the above explanation, we vary the magnetic field. As the magnetic field increases, Δ decreases and thus the optimal separation decreases. In Fig. 6(b) we show the dependence of the optimal separation of the defects $2x_0$ and Δ on the magnetic field. Although they are not exactly identical, the rate of the decreasing is comparable. The slight difference in $2x_0$ and Δ is due to the fact that the defect has a finite range which tends to affect a finite area of the magnetization vector.

V. SUMMARY AND CONCLUSIONS

We have quantitatively investigated the dependence of the energy barrier on the defect potential size and strength in a simplified 1D magnetic wire. Based on Braun's analytical solution of the saddle-point untwisted wall function for an ideal film, we find that the saddle-point solution can be calculated numerically in the presence of defects. Since the energy barrier plays a critical role in thermal stability of magnetic devices, the present numerical calculation provides a step forward in treating realistic films with various pinning or defects.

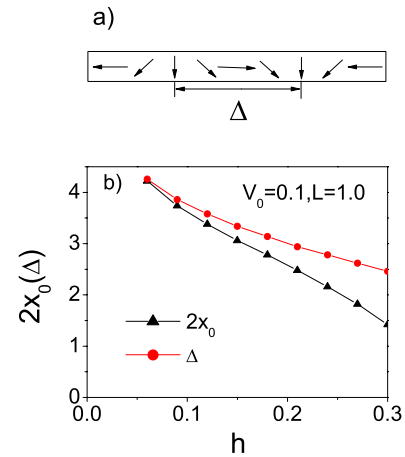Most of the quantitative results obtained in this work could be readily understood in terms of perturbation of the defect potentials on the ideal magnetic wire. The effect of two defects is most interesting. The minimum-energy barrier with respect to the separation of the two defects could be relevant to experiments in two cases. In a film with unintentional defects, the thermal reversal should first take place in the locations where the separation of the defects is approximately the size of the untwisted wall or Δ. Another case is deliberately making two notches at the edge of the film. The energy barrier would depend on the distance between the two notches, and it is possible to study the predicted energy barrier experimentally.

[1] A. Aharoni, J. Appl. Phys. **80**, 3133 (1996).

[2] W. F. Brown, Jr., Phys. Rev. **130**, 1677 (1963).

[3] S. Y. Chou, Proc. IEEE **85**, 652 (1997).

[4] H. B. Braun, Phys. Rev. Lett. **71**, 3557 (1993).

[5] H. B. Braun, Phys. Rev. B **50**, 16485 (1994).

[6] K. Martens, D. L. Stein, and A. D. Kent, Phys. Rev. B **73**, 054413 (2006).

[7] P. N. Loxley, Phys. Rev. B **77**, 144424 (2008).

[8] D. Suess, S. Eder, J. Lee, R. Dittrich, J. Fidler, J. W. Harrell, T. Schrefl, G. Hrkac, M. Schabes, N. Supper, and A. Berger, Phys.

Rev. B **75**, 174430 (2007).

[9] R. Wieser, U. Nowak, and K. D. Usadel, Phys. Rev. B **69**, 064401 (2004).

[10] A. Sokolov, R. Sabiriano, W. Wernsdorfer, and B. Doudin, J. Appl. Phys. **91**, 7059 (2002).

[11] H. Forster, T. Schrefl, W. Scholz, D. Suess, V. D. Tsiantos, and J. Fidler, J. Magn. Magn. Mater. **249**, 181 (2002).

[12] B. Hausmanns, T. P. Krome, G. Dumpich, E. F. Wassermann, D. Hinzke, U. Nowak, and K. D. Usadel, J. Magn. Magn. Mater. **240**, 297 (2002).

[13] W. Wernsdorfer, K. Hasselbach, A. Benoit, B. Barbara, B. Doudin, J. Meier, J. P. Ansermet, and D. Mailly, Phys. Rev. B **55**, 11552 (1997).

[14] L. Thomas, M. Hayashi, X. Jiang, R. Moriya, C. Rettner, and S. Parkin, Science **315**, 1553 (2007).

[15] R. L. Burden and D. Faires, *Numerical Analysis*, 7th ed. (Thomson Learning, London, 2001), p. 667.